

# Peridynamic analysis of curved elastic beams

Zhengkao Yang<sup>a</sup>, Konstantin Naumenko<sup>b,\*</sup>, Chien-Ching Ma<sup>a</sup>, Erkan Oterkus<sup>c</sup>, Selda Oterkus<sup>c</sup>

<sup>a</sup>*Department of Mechanical Engineering, National Taiwan University, Taipei, Taiwan*

<sup>b</sup>*Otto-von-Guericke-University Magdeburg, Institute of Mechanics, PF 4120, 39016, Magdeburg, Germany*

<sup>c</sup>*PeriDynamics Research Centre, Department of Naval Architecture, Ocean and Marine Engineering, University of Strathclyde, Glasgow, United Kingdom*

---

## Abstract

Peridynamics is an extended continuum theory which operates with non-local deformation measures as well as long range internal force/moment interactions. The aim of this paper is to present and to analyze peridynamic governing equations for elastic curved beams. To this end the strain energy density is formulated as a function of two non-local deformation measures including the axial deformation and curvature. Applying the Lagrangian formalism, peridynamic equations of motion are derived. To analyze curved beams of finite length peridynamic boundary conditions are required. Examples of boundary conditions including simple support and clamped edge are presented by introducing a fictitious domain. Solutions to PD equations of motion are presented for various problems including static analysis of simply supported and clamped arc beams as well as modal analysis of a slender ring and a simply supported arc beam. To validate peridynamic formulations, solutions for displacements, natural frequencies and vibration modes are compared with those by the classical beam theory. A very good agreement between the non-local and the classical theories is observed for the case of the small horizon sizes which shows the capability of the derived equations of motion and proposed boundary conditions.

*Keywords:* Peridynamics, beam theory, curved beam, modal analysis

---

## 1. Introduction

During last decades non-local continuum mechanics theories have drawn increasing interest due to many applications, such as micro- and nanometer scale components, composite materials with high contrast in material properties and laminates with extremely thin layers. One way to enhance the classical continuum mechanics (CCM) is to introduce higher order deformation gradients as arguments of the strain energy density (Bertram, 2023; Cordero et al., 2016). Applying a variational principle, a family of strain gradient theories according to a maximal order of the considered deformation gradient can be formulated. In the case of elasticity, Nth-order gradient

---

\*Corresponding author

*Email addresses:* zhengkao.yang@strath.ac.uk (Zhengkao Yang), konstantin.naumenko@ovgu.de (Konstantin Naumenko), ccma@ntu.edu.tw (Chien-Ching Ma), erkan.oterkus@strath.ac.uk (Erkan Oterkus), selda.oterkus@strath.ac.uk (Selda Oterkus)

*Preprint submitted to European Journal of Mechanics / A Solids*

*June 3, 2023*

terms lead to a system of linear or nonlinear partial differential equations of the 2Nth order (Eremeyev, 2023). Their properties are well-understood within the general theory of partial differential equations. Strain gradient theories lead to higher order stress tensors and as a result require many additional boundary conditions.

Another approach is to introduce non-local integral type strain measures as proposed within Peridynamics (PD). This type of extended continuum theory operates with long-range internal forces (Silling, 2016; Silling and Lehoucq, 2010), instead of higher order stress measures. The deformation gradient, its higher gradients or gradients of internal state variables are not introduced. Deformation of bond vectors with initially finite length are analyzed in contrast to differential line elements. The resulting PD equations of motion are of integro-differential type, opposed to strain gradient theories, where partial differential equations are derived. Properties of PD integral equations as well as corresponding analytical solutions are analyzed only for few problems.

Thin-walled structures, such as slender beams, plates and shells are obviously three-dimensional structures and can be analyzed by using three-dimensional solid mechanics. However, the application of three-dimensional PD theories to thin-walled structures generally leads to a high computational effort since many nodes over the thickness direction are required to provide accurate solutions (Naumenko et al., 2022). Furthermore, for relatively thin components, for example interlayers in laminated photovoltaic panels (Aßmus et al., 2016), the PD horizon size may be comparable with the layer thickness leading to a spurious force interaction between the plies. To overcome these problems, PD theories for beams, plates and shells are required.

By analogy with CCM, PD theories for thin-walled structures can be developed by formulating governing equations directly for deformable lines for beams, planes in the case of plates and surfaces for shells. Alternatively, three-dimensional PD equations can be reduced to one- or two-dimensional problems applying special assumptions. In Chen (2021) the PD strain energy density for a straight beam in terms of the non-local curvature is formulated. PD beam elements with six degrees of freedom at each node is developed in Shen et al. (2021b). Discretized forms of equations of motion for the axial displacement and the deflection for straight beams are presented in Shen et al. (2021a). The PD integro-differential equation of motion with respect to unknown deflection for a straight beam is derived in Yang et al. (2022a). Discretized forms of PD plate and shell equations are developed in Vazic et al. (2020) applying the Lagrange principle. A linear PD shell theory with respect to the displacements and small rotations of the base surface is developed in Chowdhury et al. (2016). Peridynamic models for fibers and membranes are proposed in Silling and Bobaru (2005). In Naumenko and Eremeyev (2022) a non-linear PD plate theory considering finite rotations is presented. PD plate points are assumed to behave like rigid bodies and non-local force and moment interactions are introduced. Governing balance laws are formulated directly for the plate. On the other hand, in Taylor and Steigmann (2015) a PD plate theory is derived as a two-dimensional approximation of the three-dimensional bond-based PD via an asymptotic analysis.

An important issue of a PD theory is the analysis of solutions as they behave by reducing the horizon size. For elastic solids the solutions should converge to those of CCM as the horizon size approaches zero. Another aspect is the influence of the type of PD constraints and boundary conditions on the results. Unlike the CCM, where many analytical solutions for beams, plates, shells and three-dimensional solids are derived, only few analytical solutions to PD equations are

available in the literature. Analytical solutions for rods are presented in Mikata (2012); Nishawala and Ostoja-Starzewski (2017); Silling et al. (2003); Weckner and Abeyaratne (2005). For initially straight beams with various boundary constraints series solutions to PD equations are given in Yang et al. (2022b). Governing PD equations for buckling of straight beams are derived in Yang et al. (2022a). For several types of boundary conditions explicit expressions for the buckling loads are presented. Analytical solutions of peristatics and peridynamics for three-dimensional infinite media for an arbitrary body force density, and arbitrary initial conditions are obtained in Mikata (2019, 2023).

Analytical solutions presented in the literature illustrate the effect of non-locality, in particular the influence of PD horizon size on the deformation, explicitly. Furthermore, analytical solutions are useful to validate the numerical methods, such as the PD meshfree method (Silling and Askari, 2005), PD codes, such as Peridigm (Littlewood et al., 2023) and to analyze the convergence of numerical results (Seleson and Littlewood, 2016).

The aim of this study is to derive the governing equations for initially curved linear-elastic beams within the PD framework. To this end the strain energy densities corresponding to the axial extension and the bending of the beam will be formulated in terms of non-local PD deformation measures. Applying the Lagrangian formalism, novel PD equations of motion for curved beams will be derived. For the special cases of straight rod and straight beam the obtained equations will be compared with those available in the literature. Examples of PD boundary conditions corresponding to the simple support and the clamped edge will be introduced.

For beams with constant curvature, novel closed form analytical solutions to PD equations of motion for both static and dynamic cases and different types of boundary conditions will be derived. Furthermore, discretized forms of equations of motion and numerical solutions will be presented. The results will be validated by comparing the derived solutions against solutions of the classical beam theory (CBT).

## 2. Peridynamic beam theory

### 2.1. Classical equations and assumptions

Figure 1 illustrates a curved beam in a reference configuration. Let  $s$  be the arc length coordinate for a point of the beam centerline and  $\mathbf{r}(s)$  the corresponding position vector. The following relations with respect to the basic geometrical parameters of the curved beam can be established, e.g. Green and Laws (1966)

$$\mathbf{t} = \frac{d\mathbf{r}}{ds}, \quad \frac{d\mathbf{t}}{ds} = -\chi\mathbf{n}, \quad \chi = \frac{1}{R}, \quad (1)$$

where  $\mathbf{t}(s)$  is the unit tangent vector,  $\mathbf{n}(s)$  is the unit normal vector,  $\chi(s)$  is the curvature and  $R(s)$  is the radius of curvature of the centerline. For the sake of brevity let us consider plane curves, such that the binormal vector  $\mathbf{b} = \mathbf{t} \times \mathbf{n}$  does not depend on  $s$ . In this case

$$\frac{d\mathbf{n}}{ds} = \chi\mathbf{t} \quad (2)$$

Furthermore, let us analyze the plane bending of the beam. In this case the deformed centerline belongs to the plane the spanned on the vectors  $\mathbf{t}$  and  $\mathbf{n}$ . In the case of small cross-sectional

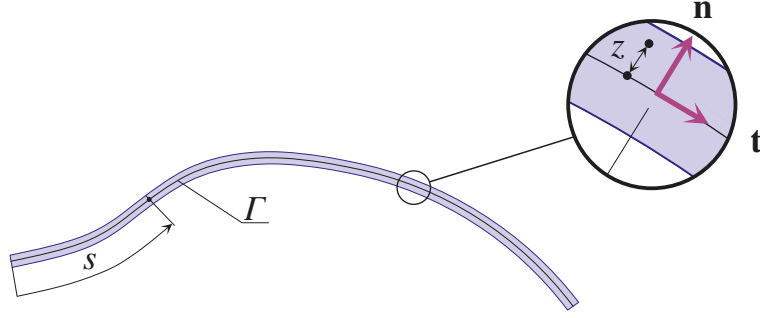


Fig. 1. Geometry and coordinates for a curved beam

rotations the displacement vector  $\mathbf{u}$  can be represented as follows

$$\mathbf{u}(s, z) = \mathbf{u}(s) + \theta(s)z\mathbf{t}(s), \quad (3)$$

where  $\mathbf{u}$  is the displacement vector of the beam centerline,  $\theta$  is the angle of cross-sectional rotation, and  $z$  is the coordinate along the normal direction, as shown in Fig. 1. The displacement vector  $\mathbf{u}$  is represented as follows

$$\mathbf{u}(s) = u(s)\mathbf{t}(s) + w(s)\mathbf{n}(s), \quad (4)$$

with  $u$  being the axial and  $w$  the normal displacement, respectively.

Assuming small strains the linear strain tensor  $\boldsymbol{\varepsilon}$  is related to the displacement field by the following equation

$$\boldsymbol{\varepsilon} = \frac{1}{2} \left( \nabla \mathbf{u} + (\nabla \mathbf{u})^T \right), \quad \nabla(\dots) = \frac{1}{1 + \chi z} \mathbf{t} \frac{\partial(\dots)}{\partial s} + \mathbf{n} \frac{\partial(\dots)}{\partial z} \quad (5)$$

Inserting Eqs (3) and (4) into Eq. (5) the strain tensor is computed as follows

$$\boldsymbol{\varepsilon} = \varepsilon \mathbf{t} \otimes \mathbf{t} + \frac{1}{2} \gamma (\mathbf{t} \otimes \mathbf{n} + \mathbf{n} \otimes \mathbf{t}), \quad (6)$$

with the following expressions for normal strain  $\varepsilon$  and the transverse shear strain  $\gamma$

$$\varepsilon = \frac{1}{1 + \chi z} \left( \frac{du}{ds} + z \frac{d\theta}{ds} + \chi w \right), \quad \gamma = \frac{1}{1 + \chi z} \left( \theta + \frac{dw}{ds} - \chi u \right) \quad (7)$$

For the shear rigid beams  $\gamma = 0$  is assumed, resulting in

$$\theta = -\frac{dw}{ds} + \chi u, \quad \varepsilon = \frac{1}{1 + \chi z} \left[ \frac{du}{ds} + \chi w + z \left( -\frac{d^2w}{ds^2} + \chi \frac{du}{ds} + u \frac{d\chi}{ds} \right) \right] \quad (8)$$

Considering slender beams,  $|z|/R \ll 1$  and Eq. (8) simplifies to

$$\varepsilon = \frac{du}{ds} + \chi w + z \left( -\frac{d^2w}{ds^2} + \chi \frac{du}{ds} + u \frac{d\chi}{ds} \right) \quad (9)$$

For the linear-elastic material behaviour the strain energy per unit length is defined as follows

$$W = \frac{1}{2} \int_A E \varepsilon^2 dA, \quad (10)$$

where  $E$  is the Young's modulus and  $A$  is the cross-sectional area. With Eq. (9) the strain energy density (10) takes the following form

$$W = W_e + W_b, \quad W_e = \frac{EA}{2} \epsilon^2, \quad W_b = \frac{EI}{2} \kappa^2, \quad \epsilon = \frac{du}{ds} + \chi w, \quad \kappa = -\frac{d^2w}{ds^2} + \chi \frac{du}{ds} + u \frac{d\chi}{ds}, \quad (11)$$

where  $W_e$  and  $W_b$  are the strain energy densities with respect to the axial extension and bending, respectively, and  $I$  is the second area moment of the beam cross section.

## 2.2. Peridynamic equations of motion

Unlike the CCM and the classical beam theory (CBT) where strains are defined in terms of derivatives with respect to the coordinates, non-local deformation measures are introduced in the PD framework. The PD deformations can be introduced as work conjugates to the bond force and moment densities considering the energy balance equation, e.g. Naumenko and Eremeyev (2022); Silling and Lehoucq (2010). For elastic structures a class of PD theories can be derived assuming the correspondence of the strain energy density from the CCM as a function of the PD deformation measures Yang et al. (2022a,b,c).

Let  $\Gamma$  be the collection of points of the beam centerline, Fig. 1. Introduce the PD horizon as an open ball centered at point  $s$  with radius of the PD horizon size  $\delta$  defined  $\forall s \in \Gamma$ , i.e.

$$H_s := \{s' \in \Gamma : |s' - s| < \delta\} \quad (12)$$

In PD, the strain energy density of any arbitrary material point  $s$  depends upon both the displacement of itself and the displacement fields within its horizon  $H_s$ , i.e.

$$\bar{W}(s) = \bar{W}(\mathbf{u}(H_s)) \quad (13)$$

To formulate the PD strain energy density consider the following Taylor expansions for  $u$  and  $w$

$$u(s') - u(s) = \left. \frac{du}{ds} \right|_s (s' - s) + O(|s' - s|^2), \quad \chi(s) \frac{w(s') + w(s)}{2} = \chi(s)w(s) + O(|s' - s|) \quad (14)$$

Adding Eq. (14)<sub>1</sub> with (14)<sub>2</sub>, squaring both sides and integrating over the PD horizon of material point  $s$ , by taking into account (11)<sub>4</sub> and ignoring terms of higher order the following equation can be obtained

$$\int_{s-\delta}^{s+\delta} \frac{1}{|s' - s|} \left( u(s') - u(s) + \chi(s) \frac{w(s') + w(s)}{2} (s' - s) \right)^2 ds' = \epsilon(s)^2 \int_{s-\delta}^{s+\delta} \frac{(s' - s)^2}{|s' - s|} ds' \quad (15)$$

which gives

$$\overline{\epsilon(s)^2} = \frac{1}{\delta^2} \int_{s-\delta}^{s+\delta} \frac{1}{|s'-s|} \left( u(s') - u(s) + \chi(s) \frac{w(s') + w(s)}{2} (s' - s) \right)^2 ds' \quad (16)$$

With (16) the PD extension strain energy density is formulated as follows

$$\overline{W}_e(s) = \frac{EA}{2} \frac{1}{\delta^2} \int_{s-\delta}^{s+\delta} \frac{1}{|s'-s|} \left( u(s') - u(s) + \chi(s) \frac{w(s') + w(s)}{2} (s' - s) \right)^2 ds' \quad (17)$$

It can be shown that for  $\delta \rightarrow 0$  the classical extension strain energy density (11)<sub>2</sub> can be recovered from Eq. (17). To formulate the bending part of the strain energy density consider the following expansions

$$\begin{aligned} w(s') - w(s) &= \frac{dw}{ds} (s' - s) + \frac{1}{2} \frac{d^2w}{ds^2} (s' - s)^2 + O(|s' - s|^3), \\ \chi(s) [u(s') - u(s)] &= \chi(s) \frac{du}{ds} (s' - s) + O(|s' - s|^2), \\ \mu(s) \frac{u(s') + u(s)}{2} &= \mu(s)u(s) + O(|s' - s|), \end{aligned} \quad (18)$$

where

$$\mu = \frac{d\chi}{ds}$$

By adding Eqs (18)<sub>1</sub>, (18)<sub>2</sub> and (18)<sub>3</sub>, and integrating over the PD horizon we obtain

$$\overline{\kappa}(s) = \frac{1}{2\delta} \int_{s-\delta}^{s+\delta} \left[ \mu(s) \frac{u(s') + u(s)}{2} + \chi(s) \frac{u(s') - u(s)}{s' - s} - 2 \frac{w(s') - w(s)}{(s' - s)^2} \right] ds' \quad (19)$$

With Eqs (19) and (11)<sub>3</sub> the PD bending strain energy density is formulated as follows

$$\overline{W}_b(s) = \frac{1}{2} \frac{EI}{4\delta^2} \left[ \int_{s-\delta}^{s+\delta} \left[ \mu(s) \frac{u(s') + u(s)}{2} + \chi(s) \frac{u(s') - u(s)}{s' - s} - 2 \frac{w(s') - w(s)}{(s' - s)^2} \right] ds' \right]^2 \quad (20)$$

The PD equations of motion for the beam can be derived by the Lagrangian formalism. Applied to the considered curved beam it leads to the following Euler-Lagrange equations

$$\frac{d}{dt} \frac{\partial L}{\partial \dot{u}} - \frac{\partial L}{\partial u} = 0, \quad \frac{d}{dt} \frac{\partial L}{\partial \dot{w}} - \frac{\partial L}{\partial w} = 0, \quad (21)$$

where  $L = T - U$  is the Lagrangian. The kinetic energy  $T$  is defined as follows

$$T = \frac{1}{2} \int_0^l \rho A (\dot{u}^2 + \dot{w}^2) ds \quad (22)$$

in which  $\rho$  is the density and  $l$  is the length of the beam. The potential energy  $U$  is

$$U = \int_0^l [\bar{W}_e(s) + \bar{W}_b(s)] ds - \int_0^l [p(s)u(s) + q(s)w(s)] ds, \quad (23)$$

where  $p(s)$  and  $q(s)$  are the distributed axial and lateral loads, respectively. With Eqs (17) and (20) – (23) the following equations of motion are derived

$$\begin{aligned} \rho A \ddot{u}(s) = & \frac{EA}{\delta^2} \int_{s-\delta}^{s+\delta} \frac{1}{|s'-s|} \left\{ 2[u(s') - u(s)] + [\chi(s) + \chi(s')] \frac{w(s') + w(s)}{2} (s' - s) \right\} ds' \\ & + \frac{EI}{4\delta^2} \int_{s-\delta}^{s+\delta} \left\{ \left[ -\frac{1}{2}\mu(s) + \frac{\chi(s)}{s'-s} \right] \int_{s-\delta}^{s+\delta} \Psi(\eta, s) d\eta + \left[ -\frac{1}{2}\mu(s') + \frac{\chi(s')}{s'-s} \right] \int_{s'-\delta}^{s'+\delta} \Psi(\eta, s') d\eta \right\} ds' + p(s), \end{aligned} \quad (24)$$

$$\begin{aligned} \rho A \ddot{w}(s) = & -\frac{EA}{2\delta^2} \int_{s-\delta}^{s+\delta} \frac{s'-s}{|s'-s|} \{ [\chi(s') + \chi(s)] [u(s') - u(s)] \} ds' \\ & - \frac{EA}{2\delta^2} \int_{s-\delta}^{s+\delta} \frac{s'-s}{|s'-s|} \left\{ [\chi^2(s) + \chi^2(s')] \frac{w(s') + w(s)}{2} (s' - s) \right\} ds' \\ & + \frac{EI}{4\delta^2} \int_{s-\delta}^{s+\delta} \frac{1}{(s'-s)^2} \left\{ \int_{s-\delta}^{s+\delta} \Psi(\eta, s) d\eta - \int_{s'-\delta}^{s'+\delta} \Psi(\eta, s') d\eta \right\} ds' + q(s), \end{aligned} \quad (25)$$

where

$$\begin{aligned} \Psi(\eta, s) = & \mu(s) \frac{u(\eta) + u(s)}{2} + \chi(s) \frac{u(\eta) - u(s)}{\eta - s} - 2 \frac{w(\eta) - w(s)}{(\eta - s)^2}, \\ \Psi(\eta, s') = & \mu(s') \frac{u(\eta) + u(s')}{2} + \chi(s') \frac{u(\eta) - u(s')}{\eta - s'} - 2 \frac{w(\eta) - w(s')}{(\eta - s')^2} \end{aligned}$$

In particular, by setting  $\chi = 0$  and  $q = 0$ , PD equation of motion for the axially loaded straight rod follows from Eqs (24) and (25). With  $s = x$ , where  $x$  is the coordinate along the rod axis, we obtain

$$\rho A \ddot{u} = \frac{2EA}{\delta^2} \int_{x-\delta}^{x+\delta} \frac{u(x') - u(x)}{|x' - x|} dx' + p \quad (26)$$

Solutions to Eq. (26) are presented in Mikata (2012); Silling et al. (2003) among others. With  $\chi = 0$ ,  $p = 0$  and  $s = x$  the PD equation of motion for the straight beam under transverse load is derived from Eqs (24) and (25) as follows

$$\rho A \ddot{w} = \frac{EI}{\delta^2} \int_{x-\delta}^{x+\delta} \frac{1}{(x' - x)^2} \left\{ \int_{x-\delta}^{x+\delta} \frac{w(\eta) - w(x)}{(x - \eta)^2} d\eta - \int_{x'-\delta}^{x'+\delta} \frac{w(\zeta) - w(x')}{(\zeta - x')^2} d\zeta \right\} dx' + q \quad (27)$$

Solutions to Eq. (27) are presented in Yang et al. (2022b).

For curved beams with constant curvature  $\chi = 1/R = \text{const}$  the angular coordinate  $\alpha$  can be introduced such that  $s = \alpha R$ . In this case Eqs (24) and (25) reduce to

$$\begin{aligned} \rho A \ddot{u} = & \frac{2EA}{\delta^2} \int_{\alpha-\delta/R}^{\alpha+\delta/R} \left\{ \frac{u(\alpha') - u(\alpha)}{|\alpha' - \alpha|} + \frac{w(\alpha') + w(\alpha)}{2} \text{sgn}(\alpha' - \alpha) \right\} d\alpha' \\ & + \frac{EI}{4R\delta^2} \int_{\alpha-\delta/R}^{\alpha+\delta/R} \frac{1}{R(\alpha' - \alpha)} \left\{ \begin{aligned} & \int_{\alpha-\delta/R}^{\alpha+\delta/R} \frac{(\eta - \alpha) [u(\eta) - u(\alpha)] - 2 [w(\eta) - w(\alpha)]}{(\alpha - \eta)^2} d\eta \\ & + \int_{\alpha'-\delta/R}^{\alpha'+\delta/R} \frac{(\zeta - \alpha') [u(\zeta) - u(\alpha')] - 2 [w(\zeta) - w(\alpha')]}{(\alpha' - \zeta)^2} d\zeta \end{aligned} \right\} d\alpha' + p, \end{aligned} \quad (28)$$

$$\begin{aligned} \rho A \ddot{w} = & -\frac{EA}{\delta^2} \int_{\alpha-\delta/R}^{\alpha+\delta/R} \frac{\alpha' - \alpha}{|\alpha - \alpha'|} \left\{ u(\alpha') - u(\alpha) + \frac{w(\alpha') + w(\alpha)}{2} (\alpha' - \alpha) \right\} d\alpha' \\ & + \frac{EI}{2\delta^2} \int_{\alpha-\delta/R}^{\alpha+\delta/R} \frac{1}{R^2 (\alpha - \alpha')^2} \left\{ \begin{aligned} & - \int_{\alpha-\delta/R}^{\alpha+\delta/R} \frac{(\eta - \alpha) [u(\eta) - u(\alpha)] - 2 [w(\eta) - w(\alpha)]}{(\alpha - \eta)^2} d\eta \\ & + \int_{\alpha'-\delta/R}^{\alpha'+\delta/R} \frac{(\zeta - \alpha') [u(\zeta) - u(\alpha')] - 2 [w(\zeta) - w(\alpha')]}{(\zeta - \alpha')^2} d\zeta \end{aligned} \right\} d\alpha' + q \end{aligned} \quad (29)$$

### 2.3. Boundary conditions

Equations of motion (24) and (25) are applicable for material points embedded in the PD influence domain. For material points adjacent to boundaries whose PD influence domain is defective, interactions with the environment, such as constraints or force/moment interactions must be considered. To this end a fictitious material region can be introduced. Following the approach presented in Yang et al. (2022a,b) we set the length of the fictitious region as of the PD horizon size,  $2\delta$ . For the curved beam the following examples of constraints will be analyzed.

#### 2.3.1. Simple support

Suppose the beam is simply supported at the left end with  $s = 0$ . In the case of the fixed support according to the classical theory the axial displacement, the deflection and the curvature change must be zero, i.e.

$$\begin{cases} u(0) = 0, & w(0) = 0, \\ \chi(0) \frac{du}{ds} \Big|_{s=0} - \frac{d^2w}{ds^2} \Big|_{s=0} = 0 \end{cases} \quad (30)$$

For the case that the support is movable in the axial direction we have

$$\begin{cases} \left. \frac{du}{ds} \right|_{s=0} = 0, & w(0) = 0, \\ \left. \frac{d^2w}{ds^2} \right|_{s=0} = 0 \end{cases} \quad (31)$$

To formulate the admissible PD boundary conditions let us apply the central difference as follows

$$\left. \frac{du}{ds} \right|_{s=0} \approx \frac{u(\Delta s) - u(-\Delta s)}{2\Delta s}, \quad \left. \frac{d^2w}{ds^2} \right|_{s=0} \approx \frac{w(\Delta s) - 2w(0) + w(-\Delta s)}{\Delta s^2} \quad (32)$$

Replacing  $\Delta s$  by  $\xi$ ,  $\xi \leq 2\delta$  the Eqs (30) and (32) yield

$$u(0) = 0, \quad w(0) = 0, \quad w(-\xi) + \frac{\chi(0)\xi}{2}u(-\xi) = -w(\xi) + \frac{\chi(0)\xi}{2}u(\xi) \quad (33)$$

In the case of the fixed support the following antisymmetric condition can be applied for the function  $u$ , as proposed in Yang et al. (2022b)

$$u(-\xi) = u(\xi) \quad (34)$$

Then for the fixed pin support the PD boundary condition can be formulated as follows

$$\begin{cases} u(0) = 0, & u(-\xi) = u(\xi), \\ w(0) = 0, & w(-\xi) = -w(\xi) + \chi(0)\xi u(\xi) \end{cases} \quad (35)$$

For the  $\chi = 0$  the boundary conditions of the straight rod with the fixed end Yang et al. (2022b) and the straight beam with the simply supported end Yang et al. (2022a) can be recovered. For the moving support Eqs (31) and (32) provide the following PD boundary conditions

$$\begin{cases} u(-\xi) = u(\xi), \\ w(0) = 0, & w(-\xi) = -w(\xi) \end{cases} \quad (36)$$

### 2.3.2. Clamped end

Assume that the cross section  $s = 0$  is clamped. In the classical continuum beam theory

$$\begin{cases} u(0) = 0, & w(0) = 0, \\ \left. \frac{dw}{ds} \right|_{s=0} = 0 \end{cases} \quad (37)$$

Taking into account the central difference (32) and the antisymmetry condition (34) the following PD boundary conditions of the clamped edge can be applied

$$\begin{cases} u(0) = 0, & u(-\xi) = u(\xi), \\ w(0) = 0, & w(-\xi) = w(\xi) \end{cases} \quad (38)$$

#### 2.4. Discretized equations of motion

To solve PD equations of motion a mesh-free approach can be applied, as originally proposed in Silling and Askari (2005). The beam axis is discretized by  $n$  nodes with the coordinates  $s_{(k)}$ ,  $k = 1, 2, \dots, n$ . For the sake of brevity let us formulate the discretized form of Eqs (24) and (25) for the case of constant curvature. For the  $k$ -th node we obtain

$$\begin{aligned} \rho A \ddot{u}_{(k)} = & \frac{2EA}{\delta^2} \sum_j \frac{1}{|\xi_{(j)(k)}|} \left[ (u_{(j)} - u_{(k)}) + \chi \frac{w_{(j)} + w_{(k)}}{2} \xi_{(j)(k)} \right] \Delta s_{(j)} \\ & + \frac{EI}{4\delta^4} \sum_j \frac{\chi}{\xi_{(j)(k)}} \left[ \sum_{i^k} \left( \chi \frac{u_{(i^k)} - u_{(k)}}{\xi_{(i^k)(k)}} - 2 \frac{w_{(i^k)} - w_{(k)}}{\xi_{(i^k)(k)}^2} \right) \Delta s_{(i^k)} \right. \\ & \left. + \sum_{i^j} \left( \chi \frac{u_{(i^j)} - u_{(j)}}{\xi_{(i^j)(j)}} - 2 \frac{w_{(i^j)} - w_{(j)}}{\xi_{(i^j)(j)}^2} \right) \Delta s_{(i^j)} \right] \Delta s_{(j)} + p_{(k)} \end{aligned} \quad (39)$$

$$\begin{aligned} \rho A \ddot{w}_{(k)} = & -\frac{EA}{\delta^2} \chi \sum_j \frac{\xi_{(j)(k)}}{|\xi_{(k)(j)}|} \left[ (u_{(j)} - u_{(k)}) + \chi \frac{w_{(j)} + w_{(k)}}{2} \xi_{(j)(k)} \right] \Delta s_{(j)} \\ & + \frac{EI}{4\delta^4} \sum_j \frac{2}{\xi_{(k)(j)}^2} \left[ \sum_{i^j} \left( \chi \frac{u_{(i^j)} - u_{(j)}}{\xi_{(i^j)(j)}} - 2 \frac{w_{(i^j)} - w_{(j)}}{\xi_{(i^j)(j)}^2} \right) \Delta s_{(i^j)} \right. \\ & \left. - \sum_{i^k} \left( \chi \frac{u_{(i^k)} - u_{(k)}}{\xi_{(i^k)(k)}} - 2 \frac{w_{(i^k)} - w_{(k)}}{\xi_{(i^k)(k)}^2} \right) \Delta s_{(i^k)} \right] \Delta s_{(j)} + q_{(k)} \end{aligned} \quad (40)$$

where  $f_{(k)}$  is the variable of the  $k$ -th node,  $f_{(i^k)}$  ( $i = 1, 2, \dots, n$ ) is the variable of the  $i$ -th node within the horizon of the node  $k$ ,  $\Delta s_{(k)}$  is the length of the node  $k$  and  $\xi_{(j)(k)} = x_{(k)} - x_{(j)}$ .

### 3. Examples

#### 3.1. Static analysis

In the first example we consider, slender simply supported and clamped arc beams subjected to the central lateral force  $F$ , see Fig. 2. Rectangular cross section with the height  $h = 0.01$  m and the width  $b = 0.01$  m is assumed. Beams spanned by central angle of  $\pi/2$  and radius of  $R = 1$  m are chosen. The Young's modulus  $E = 200$  GPa is specified for both cases.

By neglecting the inertia terms Eqs (39) and (40) are solved numerically. To this end the axis of the arc beam has been discretized into 101 points. The length of the nodes is  $\Delta s = R\pi/200$ . The peridynamic horizon is chosen as  $\delta = 3\Delta s$ . Outside of the each boundary 6 fictitious points were introduced to specify the constraints. The same problem is solved by ANSYS finite element code applying BEAM188 elements. A uniform finite element mesh with 100 elements along the axis of the arc was generated.

Figure 3a illustrates the axial displacement as a function of the angular coordinate  $\alpha$  for the simply supported beam arc. The normal displacement vs the location is illustrated in Fig. 3b. Displacements vs angular coordinate diagrams for the clamped beam arc are shown in Fig 4. For

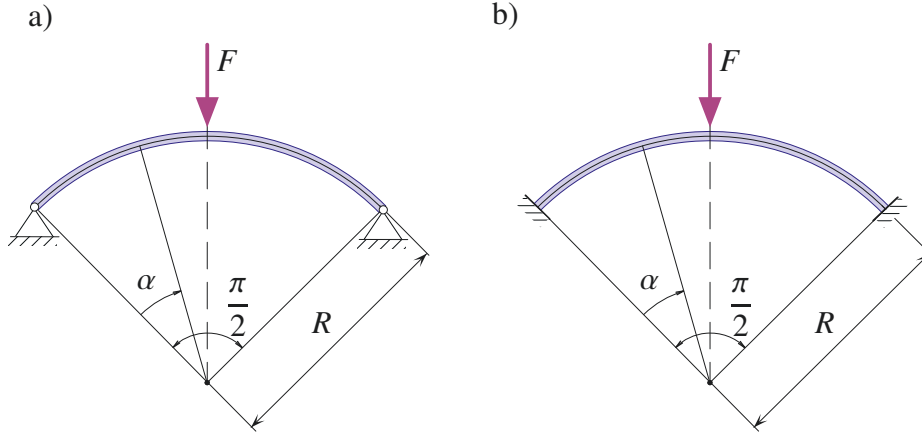


**Fig. 2.** Arc beams under static transverse load. a) Simply supported beam, b) clamped beam

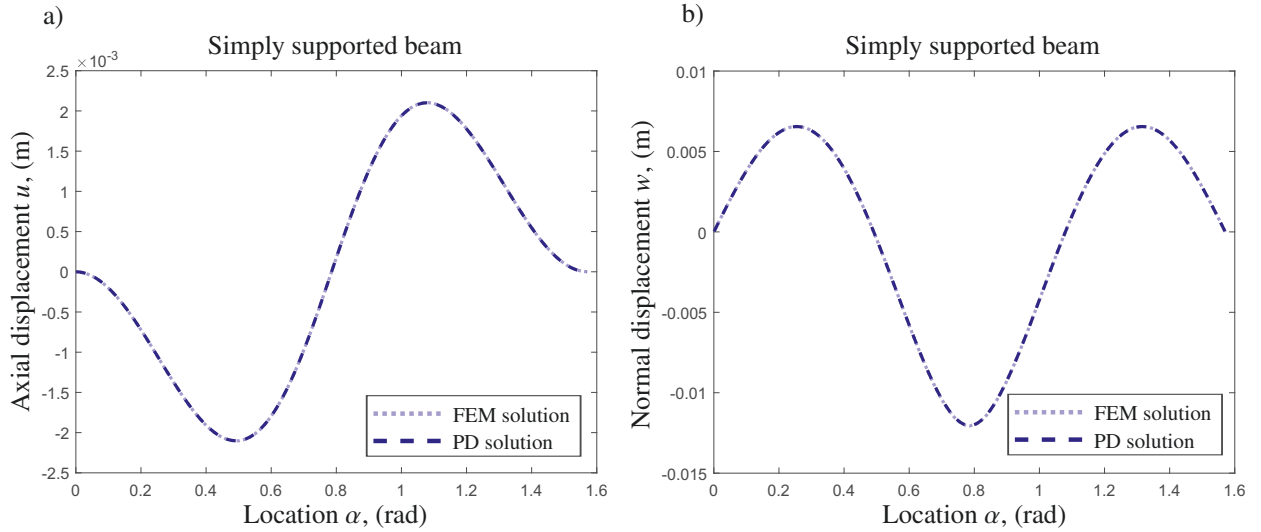


**Fig. 3.** Displacements vs axial location for simply supported circular beam arc under static load. a) Axial displacement, b) normal displacement

the comparison the solutions with the CBT and the finite element method are presented. We observe that the results based on PD equations are in a very good agreement with those obtained by the CBT and FEM.

### 3.2. Modal analysis

#### 3.2.1. Slender ring

Consider a slender ring parameterized with the radian angle coordinate  $\alpha$ . Suppose the solutions to Eqs (28) and (29) have the following forms

$$u(\alpha, t) = U_n(\alpha)e^{i\omega_n t}, \quad w(\alpha, t) = W_n(\alpha)e^{i\omega_n t}, \quad (41)$$

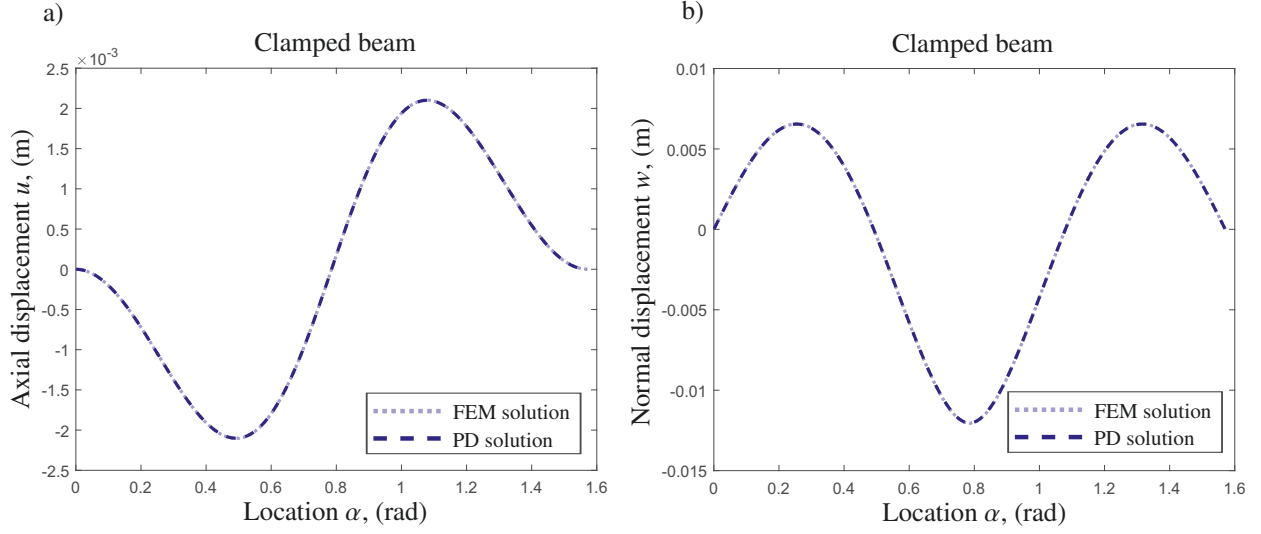


**Fig. 4.** Displacements vs axial location for clamped circular beam under static load. a) Axial displacement, b) normal displacement

where  $U_n$  and  $W_n$  are unknown functions of the coordinate and  $\omega_n$  is the natural frequency. By substituting Eqs (41) into Eqs (28) and (29) gives

$$\begin{aligned}
 -\rho A U_n(\alpha) \omega_n^2 &= \frac{2EA}{\delta^2} \int_{-\delta/R}^{\delta/R} \left\{ \frac{U_n(\alpha + \xi) - U_n(\alpha)}{|\xi|} + \frac{W_n(\alpha + \xi) + W_n(\alpha)}{2} \text{sgn}(\xi) \right\} d\xi \\
 &+ \frac{EI}{4R\delta^2} \int_{-\delta/R}^{\delta/R} \frac{1}{R\xi} \left\{ \begin{aligned} &\int_{-\delta/R}^{\delta/R} \frac{\eta [U_n(\alpha + \eta) - U_n(\alpha)] - 2 [W_n(\alpha + \eta) - W_n(\alpha)]}{\eta^2} d\eta \\ &+ \int_{-\delta/R}^{\delta/R} \frac{\zeta [U_n(\alpha + \xi + \zeta) - U_n(\alpha + \xi)] - 2 [W_n(\alpha + \xi + \zeta) - W_n(\alpha + \xi)]}{\zeta^2} d\zeta \end{aligned} \right\} d\xi
 \end{aligned} \quad (42)$$

$$\begin{aligned}
 -\rho A W_n(\alpha) \omega_n^2 &= -\frac{EA}{\delta^2} \int_{-\delta/R}^{\delta/R} \frac{\xi}{|\xi|} \left\{ [U_n(\alpha + \xi) - U_n(\alpha)] + \frac{W_n(\alpha + \xi) + W_n(\alpha)}{2} \xi \right\} d\xi \\
 &+ \frac{EI}{2\delta^2} \int_{-\delta/R}^{\delta/R} \frac{1}{R^2 \xi^2} \left\{ \begin{aligned} &-\int_{-\delta/R}^{\delta/R} \frac{\eta [U_n(\alpha + \eta) - U_n(\alpha)] - 2 [W_n(\alpha + \eta) - W_n(\alpha)]}{\eta^2} d\eta \\ &+ \int_{-\delta/R}^{\delta/R} \frac{\zeta [U_n(\alpha + \xi + \zeta) - U_n(\alpha + \xi)] - 2 [W_n(\alpha + \xi + \zeta) - W_n(\alpha + \xi)]}{\zeta^2} R d\zeta \end{aligned} \right\} d\xi
 \end{aligned} \quad (43)$$

When  $u(\alpha, t)$  vibrates at its maximum,  $w(\alpha, t)$  is at its minimum, and vice versa. Thus, the admissible functions can be selected as

$$U_n(\alpha) = a_n \sin n(\alpha - \phi), \quad W_n(\alpha) = b_n \cos n(\alpha - \phi) \quad (44)$$

By plugging Eqs (44) into Eqs (42) and (43) we obtain

$$a_n \left\{ \frac{2EA}{\delta^2} \int_{-\delta/R}^{\delta/R} \frac{\cos(n\xi) - 1}{|\xi|} d\xi - \frac{EI}{\delta^2} \frac{1}{R^2} \text{si}^2 \left( n \frac{\delta}{R} \right) + \rho A \omega_n^2 \right\} + b_n \left\{ -\frac{2EA}{\delta^2} \frac{1 - \cos(n\delta/R)}{n} + \frac{EI}{\delta^2} \frac{1}{R} \text{si} \left( n \frac{\delta}{R} \right) \int_{-\delta/R}^{\delta/R} \frac{\cos(n\eta) - 1}{\eta^2} d\eta \right\} = 0 \quad (45)$$

$$a_n \left\{ -\frac{2EA}{\delta^2} \frac{1 - \cos(n\delta/R)}{n} + \frac{EI}{2\delta^2} \int_{-\delta/R}^{\delta/R} \frac{\sin(n\xi)}{R\xi} d\xi \int_{-\delta/R}^{\delta/R} \frac{\cos(n\xi) - 1}{R\xi^2} d\xi \right\} + b_n \left\{ -\frac{EA}{2\delta^2} \int_{-\delta/R}^{\delta/R} |\xi| [\cos(n\xi) + 1] d\xi - \frac{EI}{\delta^2} \left[ \int_{-\delta/R}^{\delta/R} \frac{\cos(n\xi) - 1}{R\xi^2} d\xi \right]^2 + \rho A \omega_n^2 \right\} = 0 \quad (46)$$

which can be written into matrix system as

$$\begin{bmatrix} K_{11} + \rho A \omega_n^2 & K_{12} \\ K_{21} & K_{22} + \rho A \omega_n^2 \end{bmatrix} \begin{Bmatrix} a_n \\ b_n \end{Bmatrix} = \begin{Bmatrix} 0 \\ 0 \end{Bmatrix} \quad (47)$$

where

$$K_{11} = \frac{2EA}{\delta^2} \int_{-\delta/R}^{\delta/R} \frac{[\cos(n\xi) - 1]}{|\xi|} d\xi - \frac{EI}{\delta^2} \frac{1}{R^2} \text{si}^2 \left( n \frac{\delta}{R} \right),$$

$$K_{12} = K_{21} = -\frac{2EA}{\delta^2} \frac{1 - \cos(n\delta/R)}{n} + \frac{EI}{\delta^2} \frac{1}{R} \text{si} \left( n \frac{\delta}{R} \right) \int_{-\delta/R}^{\delta/R} \frac{\cos(n\eta) - 1}{R\eta^2} d\eta, \quad (48)$$

$$K_{22} = -\frac{EA}{2\delta^2} \int_{-\delta/R}^{\delta/R} |\xi| [\cos(n\xi) + 1] d\xi - \frac{EI}{\delta^2} \left[ \int_{-\delta/R}^{\delta/R} \frac{\cos(n\xi) - 1}{R\xi^2} d\xi \right]^2$$

For nontrivial solutions of  $a_n$  and  $b_n$

$$\det \begin{bmatrix} K_{11} + \rho A \omega_n^2 & K_{12} \\ K_{21} & K_{22} + \rho A \omega_n^2 \end{bmatrix} = 0 \quad (49)$$

The natural frequencies of a ring in PD can be obtained by solving Eq. (49).

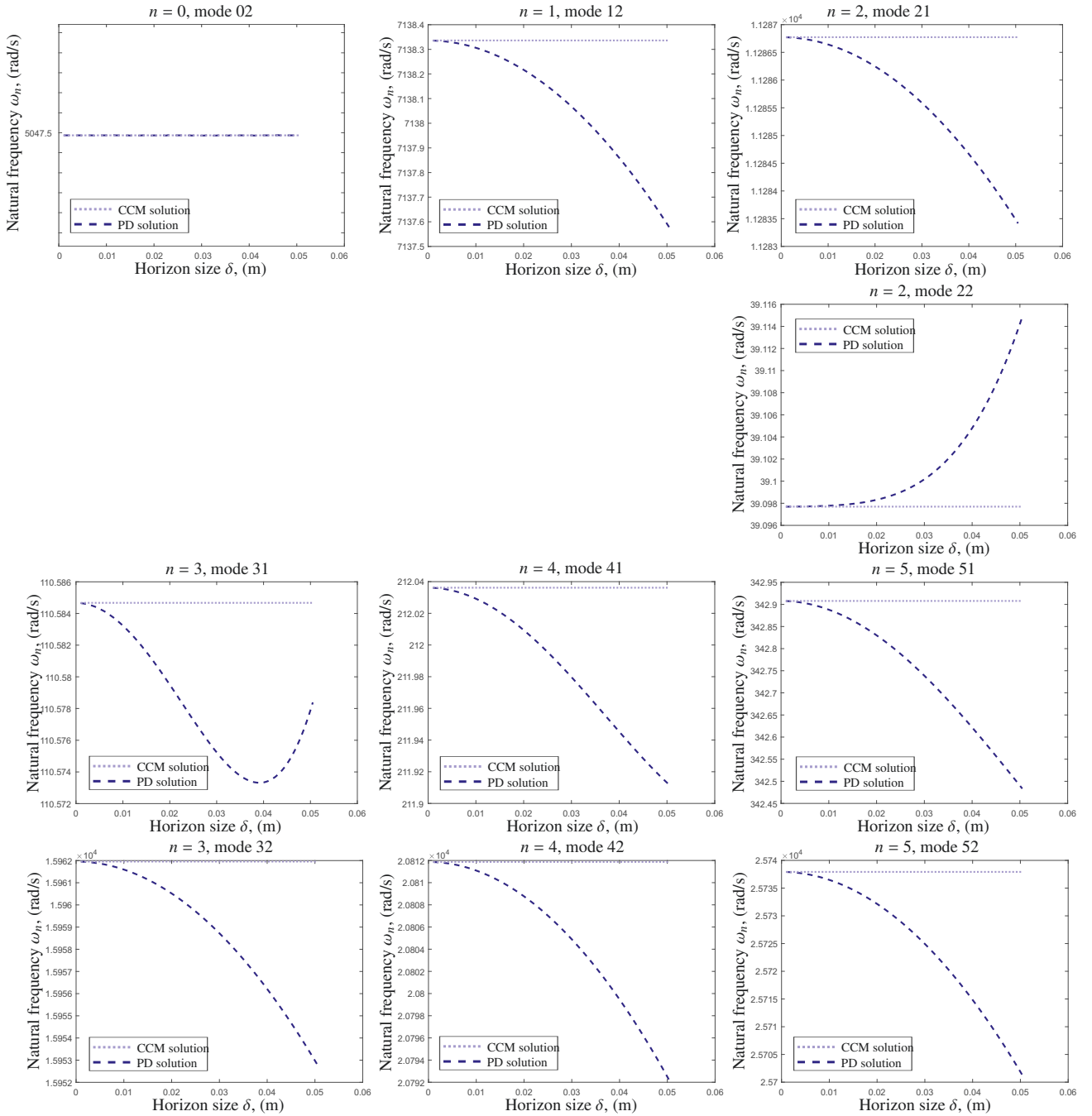
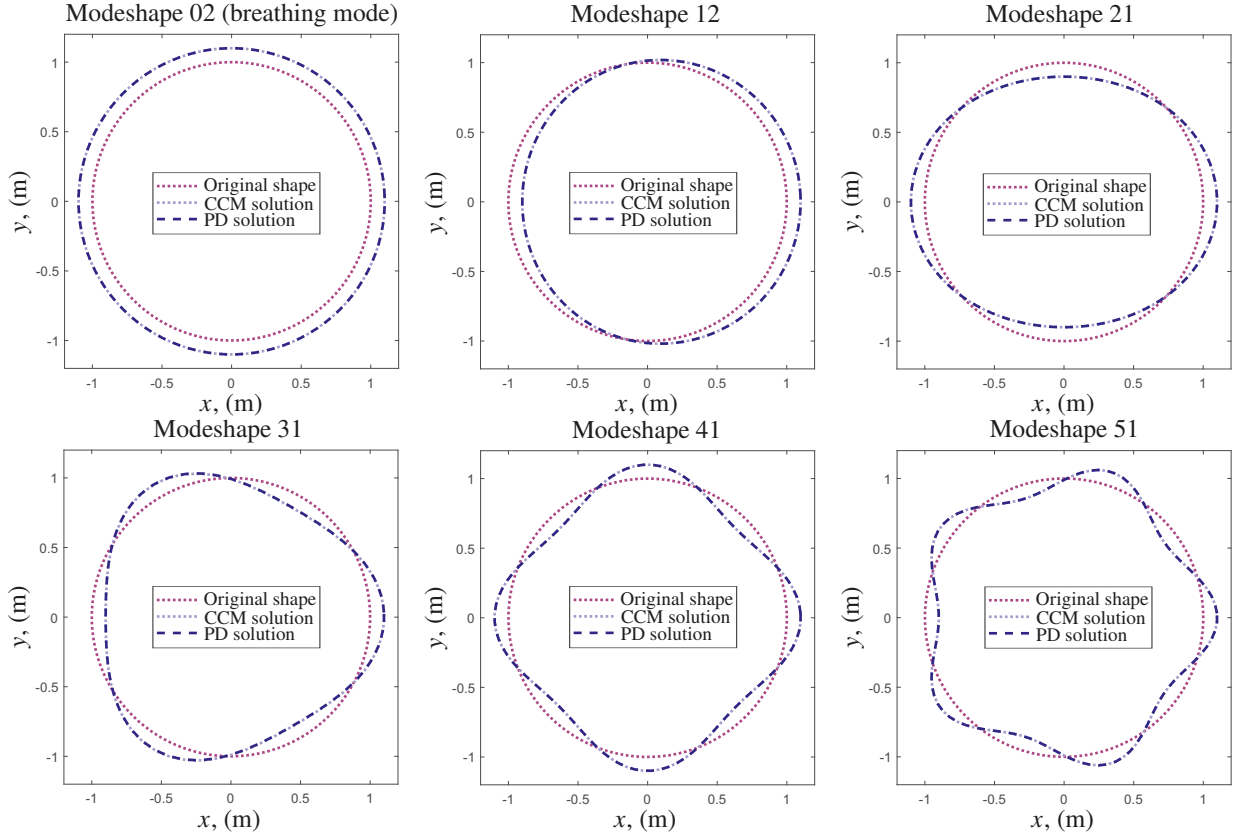


Fig. 5. Natural frequencies vs horizon size

For the numerical analysis we set  $E = 200$  GPa,  $R = 1$  m,  $\rho = 7850$  kg/m<sup>3</sup>,  $h = 0.01$  m,  $b = 0.01$  m. Figure 5 illustrates different natural frequencies of the ring as functions of the horizon size. It is obvious that results of PD and of CCM have a very good agreement when the horizon sizes are chosen as small. However, PD results deviate from those based on CCM as the horizon size



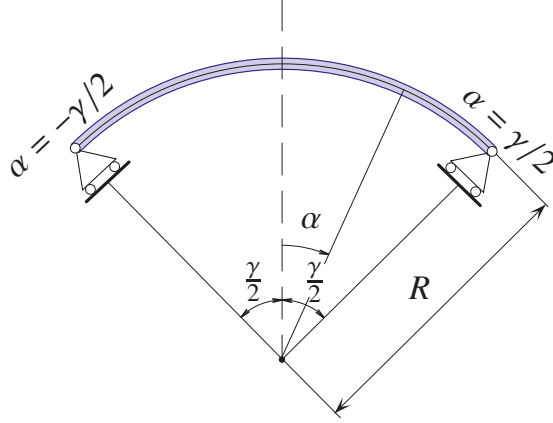
**Fig. 6.** First few modes of vibrations of a free ring (PD horizon size  $\delta=0.001$  m)

increases. This is expected since with an increase of the horizon size, nonlocal characteristics of PD start to emerge and represent a behaviour different from CCM. For small horizon size, nonlocal characteristics of PD disappear, and the results converge to those based on the local CCM theory. Figure 6 illustrates mode shapes computed by PD with the horizon size  $\delta=0.001$  m. For the comparison CCM solutions are presented. We observe that PD solutions agree well with the solutions based on CCM.

### 3.2.2. Roller simply supported arc beam

For the roller simply supported arc beam shown in the Fig. 7 the solution can be chosen by replacing  $n$  with  $\frac{n\pi}{\gamma}$  and eliminating the phase angle in Eq. (44) such that

$$U_n(\alpha) = a_n \sin \frac{n\pi\alpha}{\gamma}, \quad W_n(\alpha) = b_n \cos \frac{n\pi\alpha}{\gamma} \quad (50)$$


**Fig. 7.** Roller simply supported arc beam

Thus, the corresponding eigenvalue formulations become

$$\begin{aligned}
 & a_n \left[ \frac{2EA}{\delta^2} \int_{-\delta/R}^{\delta/R} \frac{\cos \frac{n\pi\xi}{\gamma} - 1}{|\xi|} d\xi - \frac{EI}{\delta^2} \frac{1}{R^2} \text{si}^2 \left( \frac{n\pi\delta}{R\gamma} \right) + \rho A \omega_n^2 \right] \\
 & + b_n \left\{ -\frac{EA}{\delta^2} \frac{2\gamma}{n\pi} \left( 1 - \cos \frac{n\pi\delta}{R\gamma} \right) + \frac{EI}{\delta^2} \frac{1}{R} \text{si} \left( \frac{n\pi\delta}{R\gamma} \right) \int_{-\delta/R}^{\delta/R} \frac{\cos \frac{n\pi\xi}{\gamma} - 1}{\xi^2} d\xi \right\} = 0
 \end{aligned} \quad (51)$$

$$\begin{aligned}
 & a_n \left[ -\frac{EA}{\delta^2} \frac{2\gamma}{n\pi} \left( 1 - \cos \frac{n\pi\delta}{R\gamma} \right) + \frac{EI}{\delta^2} \frac{1}{R} \text{si} \left( \frac{n\pi\delta}{R\gamma} \right) \int_{-\delta/R}^{\delta/R} \frac{\cos \frac{n\pi\xi}{\gamma} - 1}{R\xi^2} d\xi \right] \\
 & + b_n \left\{ -\frac{EI}{\delta^2} \left[ \int_{-\delta/R}^{\delta/R} \frac{1}{R\xi^2} \left( 1 - \cos \frac{n\pi\xi}{\gamma} \right) d\xi \right]^2 - \frac{EA}{2\delta^2} \int_{-\delta/R}^{\delta/R} |\xi| \left( \cos \frac{n\pi\xi}{\gamma} + 1 \right) d\xi + \rho A \omega_n^2 \right\} = 0
 \end{aligned} \quad (52)$$

The natural frequencies can be casted by solving the following equation

$$\det \begin{bmatrix} K_{11} + \rho A \omega_n^2 & K_{12} \\ K_{21} & K_{22} + \rho A \omega_n^2 \end{bmatrix} = 0 \quad (53)$$

where

$$\begin{aligned}
 K_{11} &= \frac{2EA}{\delta^2} \int_{-\delta/R}^{\delta/R} \frac{\cos \frac{n\pi\xi}{\gamma} - 1}{|\xi|} d\xi - \frac{EI}{\delta^2} \frac{1}{R^2} \text{si}^2 \left( \frac{n\pi\delta}{R\gamma} \right), \\
 K_{12} = K_{21} &= -\frac{EA}{\delta^2} \frac{2\gamma}{n\pi} \left( 1 - \cos \frac{n\pi\delta}{R\gamma} \right) + \frac{EI}{\delta^2} \frac{1}{R} \text{si} \left( \frac{n\pi\delta}{R\gamma} \right) \int_{-\delta/R}^{\delta/R} \frac{\cos \frac{n\pi\xi}{\gamma} - 1}{R\xi^2} d\xi, \\
 K_{22} &= -\frac{EI}{\delta^2} \left[ \int_{-\delta/R}^{\delta/R} \frac{1}{R\xi^2} \left( 1 - \cos \frac{n\pi\xi}{\gamma} \right) d\xi \right]^2 - \frac{EA}{2\delta^2} \int_{-\delta/R}^{\delta/R} |\xi| \left( \cos \frac{n\pi\xi}{\gamma} + 1 \right) d\xi
 \end{aligned} \tag{54}$$

For the computations we set  $E = 200$  GPa,  $R = 1$  m,  $\rho = 7850$  kg/m<sup>3</sup>,  $h = 0.01$  m,  $b = 0.01$  m,  $\gamma = \pi/2$ . Figure 8 shows different natural frequencies of the ring as functions of the horizon size. Similar to the previous example we observe that natural frequencies depend on the horizon size. For small values of the horizon size the results based on PD and of CCM agree well. Mode shapes computed by PD with the horizon size  $\delta=0.001$  m are presented in Fig. 9. Again, PD solutions agree well with those based on CCM.

#### 4. Conclusions

In this study, initially curved elastic beams are analyzed within the framework of peridynamics. To this end the strain energy density is formulated as a function of non-local deformation measures for the axial deformation and bending. Applying the Lagrangian formalism, PD equations of motion were derived. In the special case for the straight rod and the straight beam the derived equations reduce to the equations presented in the literature. PD boundary conditions of simple support and clamped edge are introduced based on the fictitious domain approach.

Solutions to PD equations of motion are presented for various examples including deformation analysis of simply supported and clamped arc beams under static load, modal analysis of a slender ring as well as modal analysis of the simply supported arc beam. The validation of PD formulations and solutions was demonstrated by comparing the displacements, natural frequencies and vibration modes against the corresponding results by the classical beam theory. A very good agreement between the non-local and the classical theories is observed for the case of the small horizon sizes which shows the capability of the derived PD equations of motion and proposed boundary conditions.

The presented examples are useful to validate the numerical methods and numerical codes applied to solve PD equations.

#### Declaration of competing interest

The authors declare that they have no known competing financial interests or personal relationships that could have appeared to influence the work reported in this paper.

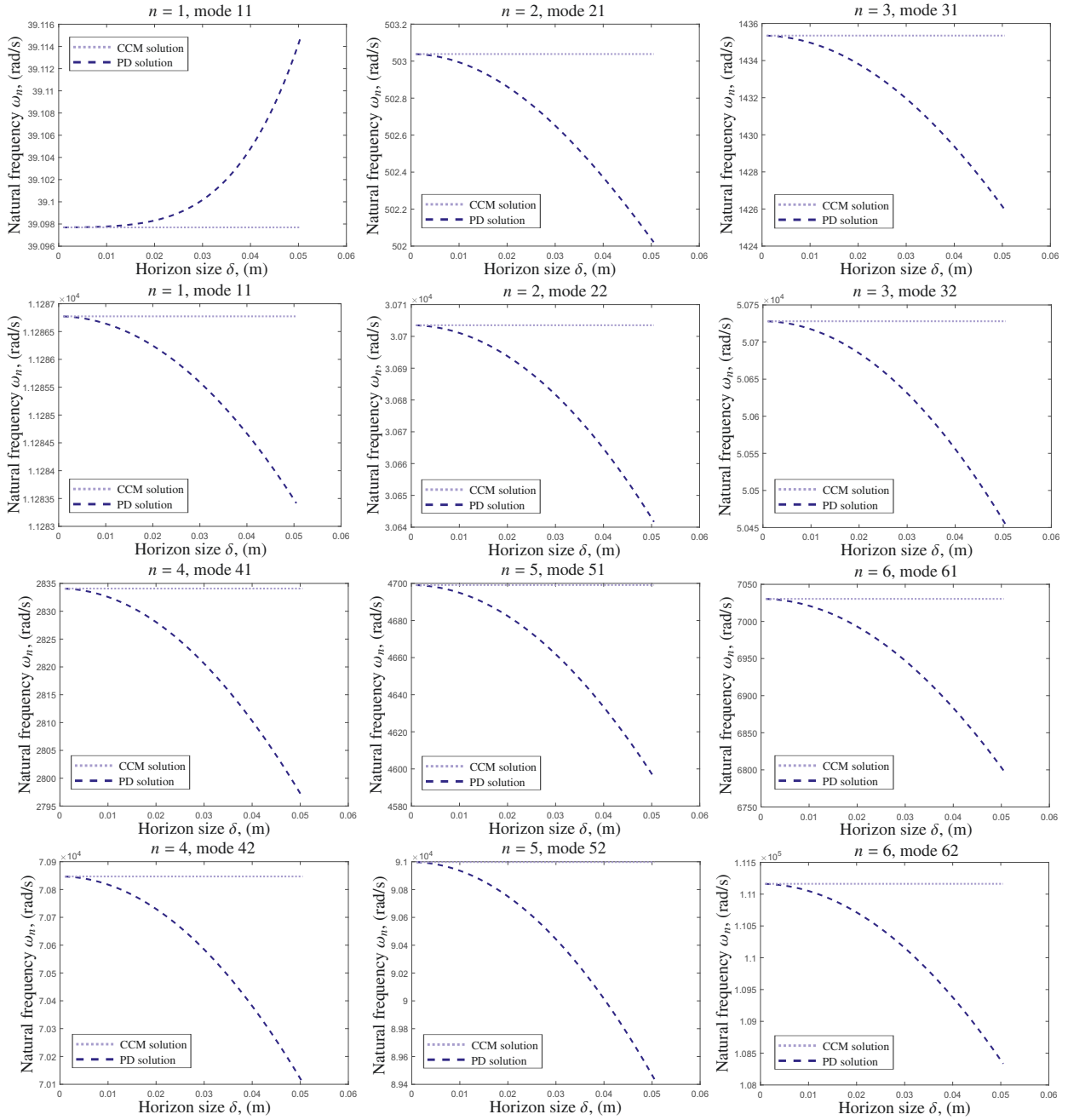
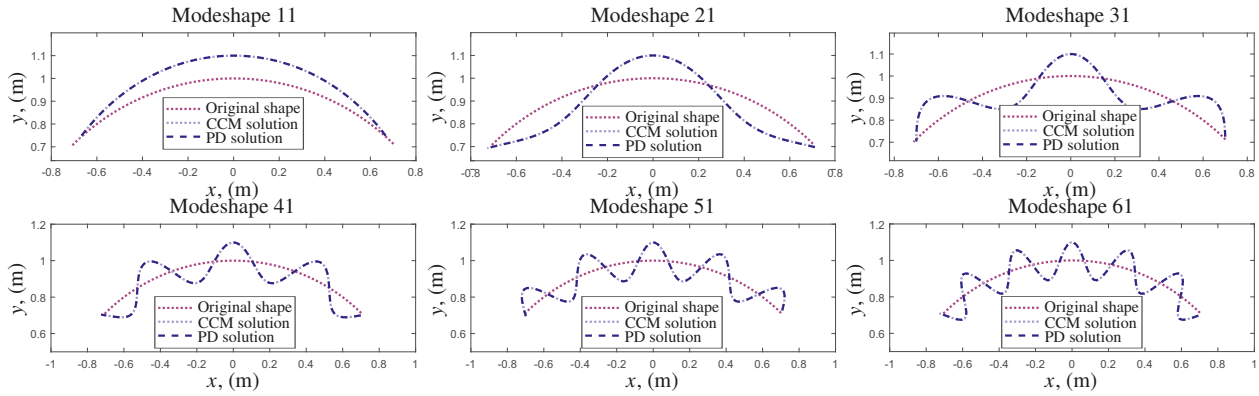


Fig. 8. Natural frequencies vs horizon size

## References

- Aβmus, M., Naumenko, K., Altenbach, H., 2016. A multiscale projection approach for the coupled global–local structural analysis of photovoltaic modules. *Composite Structures* 158, 340–358.
- Bertram, A., 2023. *Compendium on gradient materials*. Springer.
- Chen, J., 2021. *Nonlocal Euler-Bernoulli Beam Theories: A Comparative Study*. Springer.



**Fig. 9.** First few modes of vibrations of a simply supported arc with PD horizon size  $\delta=0.001$  m

- Chowdhury, S.R., Roy, P., Roy, D., Reddy, J., 2016. A peridynamic theory for linear elastic shells. *International Journal of Solids and Structures* 84, 110–132.
- Cordero, N.M., Forest, S., Busso, E.P., 2016. Second strain gradient elasticity of nano-objects. *Journal of the Mechanics and Physics of Solids* 97, 92–124.
- Eremeyev, V.A., 2023. Strong ellipticity and infinitesimal stability within  $n$ th-order gradient elasticity. *Mathematics* 11, 1024.
- Green, A.E., Laws, N., 1966. A general theory of rods. *Proceedings of the Royal Society of London. Series A. Mathematical and Physical Sciences* 293, 145–155.
- Littlewood, D.J., Parks, M.L., Foster, J.T., Mitchell, J.A., Diehl, P., 2023. The peridigm meshfree peridynamics code. *Journal of Peridynamics and Nonlocal Modeling*, 1–31.
- Mikata, Y., 2012. Analytical solutions of peristatic and peridynamic problems for a 1D infinite rod. *International Journal of Solids and Structures* 49, 2887–2897.
- Mikata, Y., 2019. Linear peridynamics for isotropic and anisotropic materials. *International Journal of Solids and Structures* 158, 116–127.
- Mikata, Y., 2023. Analytical solutions of peristatics and peridynamics for 3d isotropic materials. *European Journal of Mechanics-A/Solids*, 104978.
- Naumenko, K., Eremeyev, V.A., 2022. A non-linear direct peridynamics plate theory. *Composite Structures* 279, 114728.
- Naumenko, K., Pander, M., Würkner, M., 2022. Damage patterns in float glass plates: Experiments and peridynamics analysis. *Theoretical and Applied Fracture Mechanics* 118, 103264.
- Nishawala, V.V., Ostoja-Starzewski, M., 2017. Peristatic solutions for finite one-and two-dimensional systems. *Mathematics and Mechanics of Solids* 22, 1639–1653.
- Seleson, P., Littlewood, D.J., 2016. Convergence studies in meshfree peridynamic simulations. *Computers & Mathematics with Applications* 71, 2432–2448.
- Shen, G., Xia, Y., Hu, P., Zheng, G., 2021a. Construction of peridynamic beam and shell models on the basis of the micro-beam bond obtained via interpolation method. *European Journal of Mechanics-A/Solids* 86, 104174.
- Shen, G., Xia, Y., Li, W., Zheng, G., Hu, P., 2021b. Modeling of peridynamic beams and shells with transverse shear effect via interpolation method. *Computer Methods in Applied Mechanics and Engineering* 378, 113716.
- Silling, S.A., 2016. Introduction to peridynamics, in: *Handbook of peridynamic modeling*. Chapman and Hall/CRC, pp. 63–98.
- Silling, S.A., Askari, E., 2005. A meshfree method based on the peridynamic model of solid mechanics. *Computers & structures* 83, 1526–1535.
- Silling, S.A., Bobaru, F., 2005. Peridynamic modeling of membranes and fibers. *International Journal of Non-Linear Mechanics* 40, 395–409.
- Silling, S.A., Lehoucq, R.B., 2010. Peridynamic theory of solid mechanics. *Advances in applied mechanics* 44,

- 73–168.
- Silling, S.A., Zimmermann, M., Abeyaratne, R., 2003. Deformation of a peridynamic bar. *Journal of Elasticity* 73, 173–190.
- Taylor, M., Steigmann, D.J., 2015. A two-dimensional peridynamic model for thin plates. *Mathematics and Mechanics of Solids* 20, 998–1010.
- Vazic, B., Oterkus, E., Oterkus, S., 2020. Peridynamic model for a Mindlin plate resting on a Winkler elastic foundation. *Journal of Peridynamics and Nonlocal Modeling* , 1–10.
- Weckner, O., Abeyaratne, R., 2005. The effect of long-range forces on the dynamics of a bar. *Journal of the Mechanics and Physics of Solids* 53, 705–728.
- Yang, Z., Naumenko, K., Altenbach, H., Ma, C.C., Oterkus, E., Oterkus, S., 2022a. Beam buckling analysis in peridynamic framework. *Archive of Applied Mechanics* 92, 3503–3514.
- Yang, Z., Naumenko, K., Altenbach, H., Ma, C.C., Oterkus, E., Oterkus, S., 2022b. Some analytical solutions to peridynamic beam equations. *ZAMM-Journal of Applied Mathematics and Mechanics/Zeitschrift für Angewandte Mathematik und Mechanik* 102, e202200132.
- Yang, Z., Naumenko, K., Ma, C.C., Altenbach, H., Oterkus, E., Oterkus, S., 2022c. Some closed form series solutions to peridynamic plate equations. *Mechanics Research Communications* 126, 104000.